

## **Eigenvalues Obtained by Perturbation Exact and Numerical Methods for Short Range Potentials I**

**M.A. Abdulmomen, H.H. Aly\* and H.M.M. Mansour\*\***

*Department of Physics, King Abdulaziz University, Jeddah, Saudi Arabia*

---

ABSTRACT. We study various short range potentials and calculate their eigenvalues for both s- and p-waves using a wide range of coupling constants. We obtain these eigenvalues, first by perturbation methods, then compare these values with the ones obtained numerically and when it is possible by exact methods. Good agreements are obtained for s-waves eigenvalues and the implications for higher angular momenta eigenvalues are discussed.

### **1. Introduction**

Perturbation theories play very important roles in calculating a variety of physical quantities both classically and quantum mechanically. In quantum theory, perturbation methods are particularly useful since most of the problems do not lend themselves to exact solutions.

The perturbation method adopted in this investigation has been already applied to investigate various potential functions such as the Gauss and the Yukawa (Müller 1970 and Müller and Schilcher 1968), logarithmic (Müller-Kirsten and Bose 1978), and quark confinement power potentials (Müller-Kirsten *et al.* 1979). The method was also used to investigate multidimensional as well as multichannel

\* On leave of absence from Southern Illinois University at Edwardsville, Ill. 62026, U.S.A.

\*\* Permanent address, Department of Physics, Faculty of Science University of Cairo, Egypt.

equations (Müller-Kirsten 1979). It is felt that this particular perturbation method has features not transparent in the standard WKB approximation (Mansour and Müller-Kirsten 1982).

To obtain the Schrödinger eigenfunction using this perturbation method, we normally expand the potential function in terms of the strength of the potential. Once the eigenfunctions are obtained, it becomes an easy matter to obtain eigenvalues and other physical quantities. However, it is still important to wonder to what order of perturbation expansion, the results are meaningful and also for what value of the potential strength,  $g^2$ , or angular momentum  $l$ , we can indeed trust the perturbation series.

In this investigation (we refer to it as I), we shall use the perturbation expansion for  $g^2 \gg 1$  as was formulated by Müller (1970) and apply it to various physically realistic potential functions. To be more specific, we shall deal with regular potentials where  $\int_0^\infty rV(r)dr < \infty$  exists, and in fact this perturbation method lends itself to calculations for mildly singular and singular potentials (Aly *et al.* 1975).

We selected for our investigation three classes of potentials, the Yukawa  $\left(g^2 \frac{e^{-A^2r}}{r}\right)$ , the Gauss ( $g^2e^{-A^2r^2}$ ) and the exponential ( $g^2e^{-A^2r}$ ). The latter is the only one which is exactly solvable for the s-waves and all energy values. We shall use this potential as a good check on the range of validity of the perturbation method of Müller-Kirsten (Müller 1970).

Section (2) will include the perturbation method we are using and its further application will be discussed in section (3). In section (4), we use the numerical methods developed by Canosa and de Oliviera (1970) and Canosa (1971), and independently by Gordon (1969 and 1971). We conclude this work by discussing our results in section (5).

## 2. Solutions of the Eigenvalue Problem by Asymptotic Expansion

We start with the radial Schrödinger equation

$$\frac{d^2\psi}{dr^2} + [E - U(r)] \psi(r) = 0 \quad (1)$$

Here we consider  $\hbar = c = 2M = 1$  and  $U(r) = \frac{l(l+1)}{r^2} - V(r)$  and  $V(r)$ , the potential functions are given by

$$V_G(r) = g^2 e^{-A^2 r^2} \quad (2a)$$

$$V_y(r) = g^2 \frac{e^{-A^2 r}}{r} \quad (2b)$$

and

$$V_c(r) = g^2 e^{-A^2 r} \quad (2c)$$

We start with the Gauss potential (2a) and expand it as a power series of  $r^2$ ,

$$V(r) = g^2 \sum_{i=0}^{\infty} \frac{(-A)^{2i}}{i!} r^{2i} \quad (3)$$

following Müller-Kirsten (Müller 1970) asymptotic solutions of the Schrödinger equation in terms of (a) parabolic cylinder function for  $l = 0$ , and (b) confluent hypergeometric functions for  $l \geq 0$  can be derived. Both sets of eigenfunctions obtained are valid for values of  $r$  near the origin. A similar derivation of the asymptotic solution for large  $r$  is also needed. In this latter region, an asymptotic expansion of the Jost function was obtained and analytically continued to join the solution obtained in the neighbourhood of the origin.

As we briefly work through this perturbation method dealing with eigenvalues for  $l \geq 0$  and study the asymptotic expansion of the solutions in terms of the confluent hypergeometric functions, we realize that the program lend itself to a rather simple computational scheme to calculate all eigenvalues.

We write equation (1) in terms of the expansion given by equation (3).

$$\frac{d^2 \psi}{dr^2} + \left[ E - \frac{l(l+1)}{r^2} + g^2 - g^2 A^2 r^2 \right] \psi(r) = -g^2 \sum_{i=2}^{\infty} \frac{(-A^2)^i r^{2i}}{i!} \psi(r) \quad (4)$$

changing the independent variable to  $z = (2gA)^{-1/2} r$ , gives us

$$\frac{d^2 \psi}{dz^2} + \left[ \frac{E + g^2}{2gA} - \frac{l(l+1)}{z^2} - 1/4 z^2 \right] \psi = -1/2 \sum_{i=2}^{\infty} \left( \frac{A}{g} \right)^{i-1} \frac{(-1/2 z^2)^i}{i!} \psi \quad (5)$$

For large values of the coupling constant  $g^2$ , the right hand side of equation (5) is  $O\left(\frac{1}{g}\right)$ . Hence, the radial wave equation may be approximated by

$$\frac{d^2 \psi_0}{dz^2} + \left[ \frac{E + g^2}{2gA} - \frac{l(l+1)}{z^2} - 1/4 z^2 \right] \psi_0 = 0 \quad (6)$$

Equation (6) is a confluent hypergeometric equation whose solution (Abramowitz and Stegun 1964) is (see also Müller 1970)

$$\psi_0(z) = z^{l+1} \exp(-1/4 z^2) M(a, b; 1/2 z^2) \quad (7)$$

Setting  $q = 4n + 3$ , we have the eigenvalues

$$E = -g^2 + gA(2l + q) \quad \text{with } n = 0, 1, 2, \dots \quad (8)$$

and for equation (5), the eigenvalues are given by

$$E = -g^2 + gA(2 + q) - 2A^2\Delta \quad (9)$$

where  $\Delta$  is an expansion of  $O\left(\frac{1}{g}\right)$  (Müller 1970).

The desired eigenvalue expansion which is valid for values of  $h$   $h = -\frac{A}{g}$  and small values of  $q$  (Müller 1970), viz;

$$\begin{aligned} E = & -g^2 + gA(2l + q) - \frac{A^2}{2^4} [4(3q - 1) + 3(q^2 + 1) + 8l^2] \\ & - \frac{A^3}{2^8 \times 3g} [q(11q^2 + 1) + 2(33q^2 - 6q + 1)l + 24(5q - 1)l^2 + 64l^3] \\ & - \frac{A^4}{2^{15} \times 3g^2} [4(85q^4 + 2q^2 - 423) + l(2770q^3 - 71q^2 + 32q + 2976) \\ & + 32l^2(252q^2 - 12q + 64) + 256l^3(41q - 9) + 4096l^4] \\ & + O\left(\frac{1}{g^3}\right) \end{aligned} \quad (10)$$

Clearly for large coupling constant,  $g^2$ , equation (10) is a proper asymptotic expansion with rapidly decreasing terms.

Now we note that, as expected, the eigenvalue expansion given by equation (10) with  $l = 0$ , becomes.

$$\begin{aligned} E = & -g^2 + gqA - \frac{3A^2(q^2 + 1)}{2^4} + \frac{q(11q^2 + 1)A^2h'}{2^6 \times 3} \\ & - \frac{(85q^4 + 22q^2 - 423)A^2h^2}{2^9 \times 3} + O(h'^3) \end{aligned} \quad (11)$$

by setting  $h' = -\frac{A}{4g}$ .

The same perturbation method was also applied to the other two potential functions equations (2b) and (3c). There is, however, some modification of the perturbation method in the case of the exponential potential.

### 3. The exponential potential

Here we consider the exponential potential (equation 2c) and compare the perturbative eigenvalues obtained with those obtained from exact solution for the s-wave Schrödinger equation (1).

We start with the perturbation solution by expanding the exponential potential by writing

$$V(r) = -g^2 \left[ 1 - \frac{r}{A} + \frac{1}{2} \left( \frac{r}{A} \right)^2 + \sum_{i=3}^{\infty} \frac{(-1)^i}{i!} \left( \frac{r}{A} \right)^i \right] \quad (12)$$

Substituting this expression in equation (1) to obtain

$$\left[ \frac{d^2}{dr^2} - E + g^2 \left( 1 - \frac{r}{A} + \frac{1}{2} \left( \frac{r}{A} \right)^2 \right) \right] \psi(r) = -g^2 \left( \sum_{i=3}^{\infty} \frac{(-1)^i}{i!} \left( \frac{r}{A} \right)^i \right) \psi(r) \quad (13)$$

Putting  $\frac{z}{A} = \frac{r}{A} - 1$  and  $Z' = \frac{h}{2} z$ ,

where we define  $h = \frac{2g^2}{A^2}$  in equation (13) to obtain

$$\begin{aligned} & \left[ \frac{d^2}{dZ'^2} + \frac{A^2}{h^2} (1/2 g^2 - E) + \frac{A^4}{4} Z'^2 \right] \psi(Z') \\ &= -\frac{A^4 h^2}{2} \sum_{i=3}^{\infty} \frac{(-1)^i}{i!} \left[ 1 + i \frac{Z'}{h} + \frac{i(i-1)}{2!} \frac{Z'^2}{h^2} + \frac{i(i-1)(i-2)}{3!} \frac{Z'^3}{h^3} + \dots \right] \psi(Z') \\ &= -\frac{A^4 h^2}{2} \left[ \left( \frac{1}{e} - 1/2 \right) + \frac{Z'}{h} - \left( \frac{1}{e} \right) + \frac{Z'^2}{2h^2} \left( \frac{1}{e} - 1 \right) \right] \end{aligned}$$

$$-\frac{A^4 h^2}{2} \sum_{i=3}^{\infty} \frac{(-1)^i}{i!} \left[ \frac{i(i-1)(i-2)}{3!} \frac{Z'^3}{h^2} + \dots \right] \psi(Z') \quad (14)$$

On multiplying equation (14) by  $\sqrt{e}/A^2$  and putting

$$Z_1 = \frac{A}{e^{1/4}} Z' \quad \text{we obtain}$$

$$\left[ \frac{d^2}{dZ_1^2} + \frac{\sqrt{e}}{h^2} (1/2 g^2 - E) + \frac{\sqrt{e} h^2 A^2}{2} \left( \frac{1}{e} - 1/2 \right) + \frac{Z_1^2}{4} - \frac{AhZ_1}{2^4 \sqrt{e}} \right] \psi(Z_1) \\ = \left[ O\left(\frac{1}{h}\right) \right] \psi(Z_1) \quad (15)$$

Equation (15) can be solved by the perturbation method discussed previously in this work. The first approximation is the parabolic cylinder function  $D_{\left(\frac{q-1}{2}\right)}(Z_1)$  and for  $q = 1$  the eigenvalue is given by

$$E^{(0)} = \frac{g^2}{2e} - \frac{h^2}{2\sqrt{e}} \quad (16)$$

This solution will be compared with the exact solution previously obtained (Wu and Ohmura 1962) for the s-wave case. Since the radial Schrödinger equation (with the exponential potential) lends itself to an exact solution in terms of the Bessel functions where the physical eigenvalues can be readily obtained, we use this example as a check on the perturbation method discussed in section 2. It is important to point out that only s-wave eigenvalues can be obtained exactly. These eigenvalues are compared with those obtained by perturbation method for the s-wave case.

The exact calculation (Wu and Ohmura 1962) of eigenvalues for the exponential potential is obtained by solution of equation (1)

Here therefore we obtain,

$$\psi_n(r) = \text{const. } J_{2A^2 K_n}(\alpha e^{-r^2 A^2}) \quad (17)$$

where  $J$  is the Bessel function and  $\alpha = 2 A^2 g^2$ ,  $k^2 = E = -K^2$  for  $h = 2 M = 1$ . The eigenvalues are then given by the zeros of

$$J_{2AK}(\alpha) = 0 \quad (18)$$

For large  $g$  (large  $g^2$ ), we have

$$J_\nu(Z) = \sqrt{\frac{2}{\pi Z}} \cos(Z - 1/2 \nu\pi - 1/4 \pi); (|\arg Z| < \pi)$$

and the Zeros are given at

$$Z - 1/2 \nu\pi - 1/4 \pi = \frac{n\pi}{2}, n = 1, 3, 5, \dots$$

$$\text{or } \alpha - A k_n \pi - 1/4 \pi = 1/2 \pi \text{ for } n = 1$$

Hence, the energy eigenvalue for s-waves is

$$E = \left( \frac{2g^2}{\pi} - \frac{3}{4A} \right)^2 \quad (19)$$

#### 4. Numerical Method

The numerical methods we adopt in this work is that developed by Canosa and de Oliveira (1970) and Canosa (1971), where these authors used the method of constant steps for their sample problem while Gordon (1969, 1971) used a linear reference potential.

We shall numerically solve equation (1) with the potentials given by equations (2a) and (2b). All the potential functions we consider here vanish exponentially at infinity and the boundary conditions on the eigenfunctions are:

$$\psi(r) \rightarrow 0 \text{ as } r \rightarrow 0$$

and

$$\psi(r) \rightarrow e^{-(r\sqrt{E})} \text{ as } r \rightarrow \infty$$

We therefore may approximate the boundary condition by  $\psi(0) = \psi(R) = 0$  for sufficiently large  $R$ .

We shall refer to all these numerical methods as COG method. In this method we approximate the potential function by a step function with an arbitrary number of steps  $n$  over the interval  $0 \leq r \leq R$ . Clearly there is a large variety of step functions which may be chosen to represent the potential functions over the  $n$  subintervals

$$0 \leq r \leq r_1, r_1 \leq r \leq r_2 \dots, r_{n-1} \leq r \leq r_n = R.$$

Canosa and de Oliviera and Canosa used constant steps for their sample problems while Gordon used a linear reference potential. The former results in simple trigonometric and hyperbolic solutions, while the latter involves Airy functions or Bessel functions of order  $1/3$ . Since COG has been shown to be a second order method for a constant as well as a linear step function (Gordon 1969, 1971), we follow Canosa's and de Oliviera's formulation and represent equation (2a) by a step function with constant  $P_1, P_2, \dots, P_n$  appropriately defined in each corresponding subinterval. We need not have each subinterval of equal width. This permits us the flexibility of approximating the potential for a given number of steps  $n$  with more steps near its minimum where it varies rapidly and thereby yields a better representation of the potential function. It is important to point out that no matter what step function is selected, we can define the approximation problem to be as close to the exact problem as we wish, provided we take a large enough number of steps.

In each step, the resulting differential equation for any eigenvalue  $E$  is

$$\frac{d^2\psi}{dr^2} + (E - P_i) \psi(r) = 0, \quad i = 1, 2, \dots, n \quad (20)$$

This equation has constant coefficients and can be integrated exactly in terms of hyperbolic or trigonometric functions. Thus, in each step  $i \neq 1$  or  $n$ , the solution to equation (20) is

$$\psi(r) = A_i C(\beta_i r) + B_i S(\beta_i r) \quad (21)$$

where we define

$$\alpha_i \equiv E - P, \quad \beta_i \equiv \sqrt{|\alpha_i|}, \quad i = 2, 3, \dots, n - 1$$

In equation (21),  $A_i$  and  $B_i$  are integration constants and  $C$  and  $S$  are circular cosine and sine for  $\alpha_i > 0$  and hyperbolic cosine and sine for  $\alpha_i < 0$ , with the boundary conditions

$$\psi(0) = 0, \quad \psi(R) = 0 \text{ for sufficiently large } R$$

with this in mind, the solutions for the cases of  $i = 1$  and  $i = n$  are respectively,

$$\psi = B_1 S(\beta_1 r), \quad \psi = B_n S(\beta_n(r - R)) \quad (22)$$

Once the eigenvalues  $E$  and the integration constants are determined the problem is solved. We then obtain the eigenvalues and the corresponding eigenfunctions by matching the solutions equation (21) and equation (22) and their derivatives at the

interval boundaries. In this way, we drive a homogeneous system of  $2n - 2$  equations for  $2n - 2$  integration constants.

### 5. Conclusions

In this investigation, we used three methods to calculate various eigenvalues for a wide range of coupling constants and  $s$ - as well as  $p$ -waves. The first method, the perturbation is that developed by Müller-Kirsten, while in the numerical method we used both the uniform step function as well as the variable step function techniques, finally we solved the exponential potential exactly (section 3). The obtained eigenvalues for various coupling constants ( $g^2 \gg 1$ ) and angular momenta are summarized in the tables given here.

From Tables 1-4, one can see that the eigenvalues calculated for the Gauss potential, do not depend upon the number of steps used in the numerical calculations. This gives us confidence in the COG method by which we measure the validity of the perturbation method.

We also notice that the eigenvalues obtained depend upon the values of the coupling constant,  $g^2$ , both for  $l = 0$  and  $l = 1$  (see Tables 1-7).

**Table 1.** Eigenvalues computed by COG and perturbative method for  $l = 0$  (For Gauss Pot.)

$g^2$	Steps in COG	$E_0^{\text{COG}}$	$E_0^{P^{(a)}}$	$\delta = E_0^{\text{COG}} - E_0^P$	$\frac{\delta \times 100}{E^{\text{COG}}}$
6	500	-0.7379340	-0.7299476	-0.0079864	1.082
7	500	-1.130848	-1.123055	-0.007793	0.689
8	500	-1.567733	-1.560781	-0.006952	0.443
9	500	-2.040577	-2.034505	-0.006072	0.297
10	500	-2.543395	-2.538058	-0.005337	0.209
11	500	-3.071584	-3.066872	-0.004712	0.001
12	500	-3.621620	-3.617428	-0.004192	0.001
13	500	-4.190721	-4.186965	-0.003756	0.0008
14	500	-4.776641	-4.773258	-0.003383	0.0007
14	1000	-4.776672	-4.773258	-0.003414	0.0007
15	500	-5.377546	-5.374485	-0.003061	0.0005
15	1000	-5.377587	-5.374485	-0.003120	0.0005
16	500	-5.991916	-5.989136	-0.002780	0.0004
16	1000	-5.991967	-5.989136	-0.002831	0.0004

(a)  $q = 3$  for all eigenvalues  $E^P$  calculated with equation (10).

**Table 2.** Eigenvalues  ${}_uE^{\text{COG}}$ ,  ${}_vE^{\text{COG}}$ , with  $E^P$  for  $l = 1$  (For Gauss Pot.)

$g^2$	Steps in COG	${}_uE^{\text{COG}}$	${}_vE^{\text{COG}}$	$E^P$ <sup>(a)</sup>	$\delta_u E = {}_uE^{\text{COG}} - E^P$	$\delta_v E = {}_vE^{\text{COG}} - E^P$
14.0	500	-0.4263363	-0.4269721	-0.2567219	-0.1696144	-0.1702502
14.0	1000	-0.4269381		-0.2567219	-0.1702162	
15.0	500	-0.7197134	-0.7205267	-0.5751195	-0.1445939	-0.1454072
15.0	1000	-0.7204489		-0.5751195	-0.1453294	
16.0	500	-1.042534	-1.043505	-0.9177456	-0.124789	-0.125760
16.0	1000	-1.043405		-0.9177456	-0.125660	

(a)  $q = 3$  in equation (10) for all eigenvalues  $E^P$  calculated.(b)  $u$  is the method of uniform step function.(c)  $v$  is the variable step function.**Table 3.** Difference between eigenvalues  $E^{\text{COG}}$  and  $E^P$  for very large  $g^2$ ,  $l = 0$ <sup>(a)</sup> (For Gauss Pot.)

$g^2$	$\delta E_{0,3}^{(b)}$	$\delta E_{1,7}$	$\delta E_{2,11}$	$\delta E_{3,15}$
25	-0.00130	-0.3204714		
40	-0.00026	-0.125567		
50	-0.00017	-0.08317	(c)	
75	-0.00101	-0.04045	-0.554289	
100	-0.00156	-0.02437	-0.31260	(d)

(a) All eigenvalues calculated by COG involved  $n = 500$  steps.(b)  $E_{i,j} = E_i^{\text{COG}} - E_j^P$ ;  $i = i^{\text{th}}$  eigenvalue;  $j =$  value of  $q$  used in equation (11).(c)  $E^{\text{COG}} = 0.1973158$ ;  $E^P = +1.196081$  (unacceptable).(d)  $E^{\text{COG}} = 1.197602$ ;  $E^P = +1.038106$  (unacceptable).**Table 4.** Difference between eigenvalues  $E^{\text{COG}}$  and  $E^P$  for very large  $g^2$ ,  $l = 1$ <sup>(a)</sup>

$g^2$	$\delta E_{0,3}^{(b)}$	$\delta E_{1,7}$	$\delta E_{2,11}$
25	-0.050047		
50	-0.00629	-0.393194	
75	0.00681	-0.16188	
100	0.01527	-0.08091	-0.872626

(a) Step functions with  $n = 500$  steps was used in calculating all eigenvalues by COG method.(b)  $E_{i,j} = E_i^{\text{COG}} - E_j^P$ ;  $i = i^{\text{th}}$  eigenvalue;  $j =$  value of  $q$  used in equation (4).

With regard to the eigenvalues obtained by COG and perturbation methods, we note:

(i) For  $l = 0$ , these two methods agree quite well for all values of  $g^2$  ( $g^2 \gg 1$ ).

(ii) For  $l = 1$ , the discrepancy of the eigenvalues obtained by these different methods is quite clear. This implies that higher order perturbation corrections are needed if we were to obtain better agreements between these two methods and hence pronounce the perturbation method as a reliable tool of calculation.

**Table 5.** Yukawa potential eigenvalues  $l = 0$

$g^2$	$(E^{\text{COG}})^{(a)}$	$E^{\text{P}}$	$\delta E = E^{\text{COG}} - E^{\text{PER}}$	$\frac{\delta E \times 100}{E^{\text{COG}}}$
7	-1.652466 <sup>(2)</sup>	-1.352040	0.3000	18.15
8	-2.750715 <sup>(2)</sup>	-2.298828	0.4519	16.43
9	-4.180623 <sup>(2)</sup>	-3.484568	0.6960	16.65
	-0.17854 <sup>(3)</sup>	-0.2777233	-0.0991	55.50
10	-5.976450 <sup>(2)</sup>	-4.911251	1.0652	17.82
	-0.4511938 <sup>(3)</sup>	-0.1605551	0.2906	64.40
11	-8.177356 <sup>(2)</sup>	-6.580586	1.5968	19.53
	-0.8481445 <sup>(3)</sup>	-0.4143702	0.4338	51.16
12	-10.82700 <sup>(2)</sup>	-8.493924	2.3331	21.50
	-1.389185 <sup>(3)</sup>	-0.7812488	0.6079	43.76
13	-2.090740 <sup>(3)</sup>	-1.257231	0.8335	39.86
14	-2.966734 <sup>(3)</sup>	-1.840420	1.1263	37.95
	-0.091131 <sup>(4)</sup>	-0.1836717	-0.0925	101.50
16	-5.287964 <sup>(3)</sup>	-3.325737	-1.9622	37.10

(a) represents the  $i^{\text{th}}$  eigenvalue.

**Table 6.** Yukawa eigenvalues for  $l = 1$

$g^2$	$(E^{\text{COG}})^{(a)}$	$E^{\text{P}}$	$\delta E$	$\frac{\delta E \times 100}{E^{\text{COG}}}$
7	-1.183247 <sup>(1)</sup>	-1.089285	0.0939	7.93
8	-2.089897 <sup>(1)</sup>	-2.011719	0.0781	3.73
9	-3.329797 <sup>(1)</sup>	-3.177468	0.1523	4.57
10	-4.633302 <sup>(1)</sup>	-4.587501	0.0458	0.99
11	-6.270619 <sup>(1)</sup>	-6.242769	0.0278	0.44
13	-1.219665 <sup>(2)</sup>	-1.030159	0.1895	15.53
14	-1.779163 <sup>(2)</sup>	-1.598710	0.1804	10.14

(a) Superscript represents  $i^{\text{th}}$  eigenvalue found.

**Table 7.** Comparison of eigenvalues for the exponential potential computed exactly and by the perturbation method for  $l = 0$

$g^2$	$E_0^{\text{exact}}$	$E_0^{\text{p}}$	$\delta = (E_0^{\text{exact}} - E_0^{\text{p}})$	$\frac{\delta \times 100}{E_0^{\text{exact}}}$
6	1.124	1.457	-0.333	29.63
8	1.695	2.067	-0.372	21.95
10	2.293	2.692	-0.399	17.40
12	2.913	3.323	-0.410	14.07
14	3.546	3.964	-0.418	11.79
25	7.209	7.559	-0.350	4.85
50	16.033	15.955	+0.078	0.48
75	25.163	24.490	+0.673	2.67
100	34.457	33.094	+1.363	3.95

Here we set  $2M = 1$

(iii) Similar features appear for the Yukawa as well as the exponential potentials. The results are given in Tables 5-7.

(iv) For higher values of  $q$  (small  $l$ 's), the agreement between numerical and perturbation eigenvalues is not too good as expected (see Table 5). However, for small  $q$  (large  $l$ ) the agreement is good (see Table 6).

We may now state that although the perturbation method is handy and can produce quick results (compared with the numerical method) extreme care must be taken in order to put confidence in the obtained eigenvalues for a given range of coupling constants and a given value of angular momentum (*i.e.* higher order corrections may be needed in the perturbation expansion).

It is evident that the perturbation method does not yield very reliable eigenvalues for higher partial waves. We are currently investigating this problem and will discuss it in a future communication.

### References

- Abramowitz, M. and Stegun, I.A.** (1964) *Handbook of Mathematical Functions*, Applied Math. Series No. 55, U.S. Dept. of Commerce, National Bureau of Standards, Washington D.C.
- Aly, H.H., Müller, H.J.W. and Vahedi-Fardi** (1975) On scattering by singular potentials with a perturbation-theoretical introduction to Mathieu functions, *J. Math. Physics* **16** : 961-970.
- Canosa, J.** (1971) Numerical solution of Mathieu's equation, *J. comput. Physics* **7** : 255-272.

- Canosa, J.** and **de Oliviera, R.G.** (1970) A new method for the solution of the Schödinger equation, *J. comput. Physics* **5** : 188-207.
- Gordon, R.G.** (1969) New method for constructing wave functions for bound states and scattering, *J. Chem. Physics* **51** : 14-25.
- Gordon, R.G.** (1971) in: **Adler, B., Ferenbach, S.** and **Rotenberg, M.** (eds) *Methods in Mathematical Physics*, vol. 11, Academic press, N.Y., pp. 81-109.
- Mansour, H.M.M.** and **Müller-Kirsten, H.J.W.** (1982) Perturbative technique as alternative to WKB method applied to the double well potential, *J. Math. Physics* **23** : 1835-1845.
- Müller H.J.W.** (1970) Perturbation theory for large coupling constants applied to the Gauss potentials, *J. Math. Physics* **11** : 355-364.
- Müller, H.J.W.** and **Schilcher, K.** (1968) High Energy Scattering for Yukawa potentials, *J. Math. Physics* **19** : 255-259.
- Müller-Kirsten, H.J.W.** (1979) Multidimensional perturbation theory for nonseparable wave equations, *Physics Lett.* **A70** : 383-386.
- Müller-Kirsten, H.J.W.** and **Bose, S.K.** (1978) Solution of the wave equation for the logarithmic potential with application to particle spectroscopy, *J. Math. Physics* **20** : 2471-2480.
- Müller-Kirsten, H.J.W., Hite, C.E.** and **Bose, S.K.** (1979) Explicit solution of the wave equation for arbitrary power potentials with application to charmonium spectroscopy, *J. Math. Physics* **20** : 1878-1890.
- Wu, T.Y.** and **Ohmura, T.** (1962) *Quantum Theory of Scattering*, Prentice-Hall, Englewood Cliffs N.J.

(Received 12/02/1983;  
in revised form 08/05/1983)

## القيم الذاتية لدوال الجهد القصيرة المدى المحسوبة بطريقة نظرية الاضطرابات ، وطريقة الحل الرقمية وطريقة الحلول الكاملة

محمد أحمد عبد المؤمن ، هادى حسين علي و هشام محمد محمد منصور

قسم الفيزياء - كلية العلوم

جامعة الملك عبد العزيز - جدة - المملكة العربية السعودية

يتلخص البحث في دراسة دالات الجهد ذات المدى القصير عندما تدخل هذه الدوال في معادلة شرودنجر لغرض حساب القيم الذاتية لأمواج P,S ، حيث نفترض أن تكون قوة الدالة  $G^2$  أكبر من الواحد .

تقارن هذه القيم الذاتية التي نحصل عليها بواسطة نظرية الاضطرابات مع تلك التي حسبت بواسطة الحلول الرقمية لكلا الحالتين P,S ثم تقارن هاتان الطريقتان مع القيم الذاتية الناتجة عن الحلول الكاملة عند توفرها .

## The CdS/CuInSe<sub>2</sub> Solar Cell Interface: Thermodynamic Considerations

J.F. Wager, O.M. Jamjoum and L.L. Kazmerski

Hughes Research Laboratories, Malibu, California 90265, USA; King Abdul Aziz University, Physics Dept., Jeddah, Saudi Arabia; and Solar Energy Research Institute, 1617 Cole Blvd. Golden, Colorado 80401, USA

---

**ABSTRACT.** Simple thermodynamic arguments are used to investigate the oxidation CuInSe<sub>2</sub> and possible chemical reactions at the CdS/CuInSe<sub>2</sub> interface. Reaction products are predicted for the oxidation of CuInSe<sub>2</sub>, the oxidation of CdS, and for reactions between CdS and CuInSe<sub>2</sub>, as well as CdS and the CuInSe<sub>2</sub> native oxide. It is suggested that the oxidation of CdS is possibly associated with the partial improvement of the response of CdS/CuInSe<sub>2</sub> solar cells with annealing treatments in an oxygen ambient.

The CdS (or Cd(Zn)S)/CuInSe<sub>2</sub> solar cell efficiency is among the highest conversion efficiencies (10%, AMI) for thin-film photovoltaic devices (Chen *et al.* 1981). The device structure is composed of five layers (back metal contact, low-resistivity CuInSe<sub>2</sub>, high-resistivity CuInSe<sub>2</sub>, CdS or Cd(Zn)S-window, and top finger contact) with four internal interfaces. The electrical responses of these various metal-semiconductor and semiconductor-semiconductor interfaces have been shown to be important in determining the final cell operational parameters (Russel *et al.* 1982, and Kazmerski *et al.* 1982b). Previous surface analysis on this heterojunction have identified several reacted chemical species at the various interfaces (Kazmerski *et al.* 1982b and Kazmerski *et al.* 1981). Key to the optimum device performance is the post-fabrication heat-treatment, typically done at 200-240°C in an oxygen-containing environment. The exact effect(s) of this annealing procedure have not been identified, although the thin-film solar cells show signific-

ant increases in  $V_{oc}$  and FF – and incremental increases in efficiency of approximately 2-3%.

The purpose of this paper is to investigate the chemical interactions at the CdS-CuInSe<sub>2</sub> heterojunction, and the effects of oxygen on the Cu-ternary device using simple thermodynamic arguments. The reaction products are predicted for the oxidation of the CuInSe<sub>2</sub> and CdS, the native oxides on the Cu-ternary and the CdS-CuInSe<sub>2</sub> interface. Finally, the possible correlation between the CdS-oxidation and the improvement in cell performance are indicated.

### The Thermodynamic Approach

The basic idea behind the thermodynamic approach used in this paper is that at constant T and P, the Gibbs free energy of reaction,  $\Delta G_R$ , must be negative for a chemical reaction to be thermodynamically feasible. For several possible reactions (*i.e.*, reactions with negative values of  $\Delta G_R$ ), the reaction with the most negative value of  $\Delta G_R$  would be the most likely to occur.  $\Delta G_R$  is related to the reaction enthalpy,  $\Delta H_R$ , and entropy,  $\Delta S_R$ , by

$$\Delta G_R = \Delta H_R - T\Delta S_R \quad (1)$$

where T is temperature in degrees Kelvin. Thus  $\Delta G_R$  is composed of an energy and an entropy component. It is often difficult to obtain tabulated values of the Gibbs free energy of formation,  $\Delta G_f$ , of a given compound while the enthalpy of formation,  $\Delta H_f$ , is usually more readily available in the literature. Therefore, it is useful to approximate  $\Delta G_R$  by  $\Delta H_R$ ,

$$\Delta G_R \approx \Delta H_R \quad (2)$$

while this approximation limits the accuracy of the thermodynamic calculation, it is often used for solid state reactions occurring at relatively low temperatures (Welch 1955).  $\Delta H_R$  is calculated from the enthalpies of formation,  $\Delta H_f$ ,

$$\Delta H_R = \sum \Delta H_f (\text{products}) - \sum \Delta H_f (\text{reactants}) \quad (3)$$

The variation of the  $\Delta H_f$ 's with temperature is fairly small at relatively low temperatures and will be ignored in this analysis. Therefore, by calculating the  $\Delta H_R$ 's of various possible reactions, it is expected that the most probable reaction would be the one with the most negative  $\Delta H_R$ .

Table 1 is a list of the  $\Delta H_f^\circ$ 's used in this analysis. No value of  $\Delta H_f^\circ$  for CuInSe<sub>2</sub> has been reported in the literature, and this value was estimated by writing the two chemical reactions,



**Table 1.** Standard heats of formation,  $\Delta H_f^\circ$  at 25°C (see Dean 1979).

Substance	$\Delta H_f^\circ$ (Kcal/mole)
Cd	0
CdO	- 61.7
CdS	- 38.7
CdSO <sub>4</sub>	-223.06
CdSe	- 25*
CdSeO <sub>3</sub>	-137.5
CdSeO <sub>4</sub>	-151.3
Cu	0
CuInSe <sub>2</sub>	- 40 (a.)
CuO	- 37.6
Cu <sub>2</sub> O	- 40.3
CuS	- 12.7
Cu <sub>2</sub> S ( $\alpha$ )	- 19.0
CuSO <sub>4</sub>	-184.36
Cu <sub>2</sub> SO <sub>4</sub>	-179.6
CuSe	- 9.45
CuSe <sub>2</sub>	- 10.3
Cu <sub>2</sub> Se	- 14.2
CuSeO <sub>4</sub>	-114.36
In	0
In <sub>2</sub> O <sub>3</sub>	-221.27
InS	- 33
In <sub>2</sub> S <sub>3</sub>	-102
In <sub>2</sub> (SO <sub>4</sub> ) <sub>3</sub>	-666
InSe	- 28
In <sub>2</sub> Se <sub>3</sub>	- 82
O <sub>2</sub> (g)	0
S	0
SO <sub>3</sub> (B)	-108.63
Se	0
SeO <sub>2</sub>	- 53.86
SeO <sub>3</sub>	- 39.9
Se <sub>2</sub> O <sub>5</sub>	- 97.6

\* Kubaschewski *et al.* 1967.(a.)  $\Delta H_f^\circ$  of CuInSe<sub>2</sub> was estimated as described in the text.

Thermodynamic analysis provides insight into which reaction products will occur *in equilibrium*, if there are *no kinetic* barriers to impede the reaction from proceeding. In practice, solid-state reactions at low temperatures often are nonequilibrium phenomena which are limited by kinetics. The major reason that solid-state reactions cannot reach equilibrium is that the reactants are often diffusion-limited and cannot attain the close physical proximity of other reactants necessary to form reaction products and thereby minimize the free energy of the system.

Solid-state reactions are often modelled according to the postulate of local equilibrium (Fromhold 1976) which states that a nonequilibrium system may be conceptually divided into microscopic regions in which equilibrium thermodynamic concepts are still valid. In this paper, the postulate of local equilibrium will be implicitly applied in modelling the oxidation of  $\text{CuInSe}_2$ . This is done by specifying that Cu is diffusion-limited to the interface, and is therefore prevented from participating in the oxidation. However, it is assumed that Cu will react at the interface in a way that will minimize the local free energy.

### The Oxidation of $\text{CuInSe}_2$

#### A. Case I: Fully Oxidized $\text{CuInSe}_2$

Table 2 lists the oxidation reactions and their associated  $\Delta H_R$ 's for the situation corresponding to fully oxidized  $\text{CuInSe}_2$  where no kinetic limitations have been imposed. Notice that all the reactions have negative  $\Delta H_R$ 's and are, therefore, thermodynamically feasible. Employing the assumption that the reaction with the most negative value of  $\Delta H_R$  will be the most probable reaction indicates that the most likely reaction products are  $\text{CuSeO}_4$ ,  $\text{In}_2\text{O}_3$ , and  $\text{SeO}_2$ . However, since there are numerous approximations and sources of error inherent in this analysis, it must

**Table 2.** Fully oxidized  $\text{CuInSe}_2$ .

Reactants	Products	$\Delta H_R$ (Kcal/gm-atom)
$2\text{CuInSe}_2 + 15/2 \text{O}_2$	$\rightarrow 2\text{CuSeO}_4 + \text{In}_2\text{O}_3 + 2\text{SeO}_2$	-20.8*
$2\text{CuInSe}_2 + 13/2 \text{O}_2$	$\rightarrow 2\text{CuO} + \text{In}_2\text{O}_3 + 4\text{SeO}_2$	-20.6*
$2\text{CuInSe}_2 + 6\text{O}_2$	$\rightarrow \text{Cu}_2\text{O} + \text{In}_2\text{O}_3 + 4\text{SeO}_2$	-19.9*
$2\text{CuInSe}_2 + 8\text{O}_2$	$\rightarrow 2\text{CuSeO}_4 + \text{In}_2\text{O}_3 + \text{Se}_2\text{O}_5$	-19.5*
$2\text{CuInSe}_2 + 17/2 \text{O}_2$	$\rightarrow 2\text{CuSeO}_4 + \text{In}_2\text{O}_3 + 2\text{Se}_2\text{O}_5$	-18.0
$2\text{CuInSe}_2 + 15/2 \text{O}_2$	$\rightarrow 2\text{CuO} + \text{In}_2\text{O}_3 + 2\text{Se}_2\text{O}_5$	-17.9
$2\text{CuInSe}_2 + 7\text{O}_2$	$\rightarrow \text{Cu}_2\text{O} + \text{In}_2\text{O}_3 + 2\text{Se}_2\text{O}_5$	-17.1
$2\text{CuInSe}_2 + 17/2 \text{O}_2$	$\rightarrow 2\text{CuO} + \text{In}_2\text{O}_3 + 4\text{SeO}_3$	-15.0
$2\text{CuInSe}_2 + 8\text{O}_2$	$\rightarrow \text{Cu}_2\text{O} + \text{In}_2\text{O}_3 + 4\text{SeO}_3$	-14.2

\* Most probable reactions.

be realized that reactions with  $\Delta H_R$ 's near that of the most negative are also likely to occur. Therefore, all reactions with  $\Delta H_R$ 's within 10% of the most negative  $\Delta H_R$  (the reactions marked with an asterisk) are predicted to be possible reactions.

Since  $\Delta H_f^\circ$  for CuInSe<sub>2</sub> was approximated in a fairly crude manner, the predictions of Table 2 would appear to be of questionable accuracy. However, when values of -20 Kcal/mole and -60 Kcal/mole were used instead of -40 Kcal/mole for the  $\Delta H_f^\circ$  of CuInSe<sub>2</sub>, identical conclusions were obtained. This indicates that although the value for  $\Delta H_f^\circ$  for CuInSe<sub>2</sub> is only an estimate, the absolute value does not appear to be crucial for this prediction of relative stability.

It is useful to group the various possible reaction products of Cu, In and Se as to the most negative  $\Delta H_f^\circ$ , on a Kcal/mole basis. This is done in Table 3. Notice that the compounds with the most negative  $\Delta H_R$  (*i.e.*, CuSeO<sub>4</sub> and CuO, In<sub>2</sub>O<sub>3</sub> and SeO<sub>2</sub>) are usually the predicted reaction products.

**Table 3.**  $\Delta H_R$ 's for possible oxidation products of CuInSe<sub>2</sub>.

Substance	$\Delta H_R$ (Kcal/gm-atom)
CuSeO <sub>4</sub>	-19.1
CuO	-18.8
Cu <sub>2</sub> O	-13.4
In <sub>2</sub> O <sub>3</sub>	-44.3
SeO <sub>2</sub>	-18.0
Se <sub>2</sub> O <sub>5</sub>	-13.9
SeO <sub>3</sub>	-10.0

When there are no kinetic limitations imposed upon the oxidation process, the anticipated reaction products are just those oxides with the most negative  $\Delta H_f^\circ$ 's. Physically, this condition of no kinetic limitations will probably occur during the very first stages of oxidation when the oxygen and semiconductor atoms can easily achieve the requirement of close physical proximity. However, if there is a competition for oxygen between the Cu, In and Se atoms, the In would be expected to preferentially oxidize due to the much greater thermodynamic driving force for In oxidation (*i.e.*,  $\Delta H_f^\circ$  (In<sub>2</sub>O<sub>3</sub>) = -44.3 Kcal/gm-atom while  $\Delta H_f^\circ$  (CuSeO<sub>4</sub>, CuO, or SeO<sub>2</sub>) = -18 - 19 Kcal/gm-atom; see Table 3).

#### B. Case II: Cu Diffusion-Limited

Soon after the oxide begins to form, kinetic limitations are expected to become important since the diffusion rates of the various atoms would be expected to be

significantly different. Oxidation may proceed by diffusion of oxygen through the oxide to the semiconductor or by diffusion of semiconductor atoms through the oxide and reaction with oxygen either in the oxide or at the oxide surface. If the oxidation proceeds by indiffusion of oxygen, no kinetic diffusion limitation would be expected to occur since the oxygen would be capable of attaining close proximity to the Cu, In and Se atoms. However, oxidation often proceeds *via* outdiffusion of the semiconductor substrate atoms and subsequent oxidation.

There is evidence (Kazmerski *et al.* 1982a) that the oxidation of CuInSe<sub>2</sub> is limited by Cu outdiffusion from the semiconductor substrate. This implies that Cu cannot readily oxidize. The energetic of this situation is considered in Table 4. When this kinetic limitation is imposed, In<sub>2</sub>O<sub>3</sub> and SeO<sub>2</sub> are still expected to form as the oxide while the Cu is left behind at the interface as free, elemental Cu or it could react with Se to form either Cu<sub>2</sub>Se or CuSe. Notice that if Cu and Se were both diffusion-limited, Cu<sub>2</sub>Se would be expected to form at the interface and the oxide would be expected to be In<sub>2</sub>O<sub>3</sub>. This interfacial species has been previously reported using angular-resolved XPS for thermal oxides (Kazmerski *et al.* 1981).

**Table 4.** Cu diffusion-limited.

Reactants	Products	$\Delta H_R$ (Kcal/gm-atom)
2CuInSe <sub>2</sub> + 11/2 O <sub>2</sub>	→ 2Cu + In <sub>2</sub> O <sub>3</sub> + 4SeO <sub>2</sub>	-18.8*
2CuInSe <sub>2</sub> + 9/2 O <sub>2</sub>	→ Cu <sub>2</sub> Se + In <sub>2</sub> O <sub>3</sub> + 3SeO <sub>2</sub>	-18.7*
2CuInSe <sub>2</sub> + 7/2 O <sub>2</sub>	→ 2CuSe + In <sub>2</sub> O <sub>3</sub> + 2SeO <sub>2</sub>	-17.9*
2CuInSe <sub>2</sub> + 21/4 O <sub>2</sub>	→ Cu <sub>2</sub> Se + In <sub>2</sub> O <sub>3</sub> + 3/2Se <sub>2</sub> O <sub>5</sub>	-16.3
2CuInSe <sub>2</sub> + 4O <sub>2</sub>	→ 2CuSe + In <sub>2</sub> O <sub>3</sub> + Se <sub>2</sub> O <sub>5</sub>	-16.1
2CuInSe <sub>2</sub> + 13/2 O <sub>2</sub>	→ 2Cu + In <sub>2</sub> O <sub>3</sub> + 2Se <sub>2</sub> O <sub>5</sub>	-16.0
2CuInSe <sub>2</sub> + 3/2 O <sub>2</sub>	→ 2CuSe <sub>2</sub> + In <sub>2</sub> O <sub>3</sub>	-14.7
2CuInSe <sub>2</sub> + 9/2 O <sub>2</sub>	→ 2CuSe + In <sub>2</sub> O <sub>3</sub> + 2SeO <sub>3</sub>	-14.1
2CuInSe <sub>2</sub> + 6O <sub>2</sub>	→ Cu <sub>2</sub> Se + In <sub>2</sub> O <sub>3</sub> + 3SeO <sub>3</sub>	-13.8
2CuInSe <sub>2</sub> + 15/2 O <sub>2</sub>	→ 2Cu + In <sub>2</sub> O <sub>3</sub> + 4SeO <sub>3</sub>	-13.1

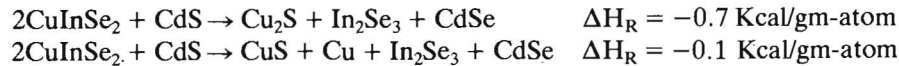
\* Most probable reactions.

Another factor which should be considered when modelling the oxidation of CuInSe<sub>2</sub> is the volatility of possible reaction products, SeO<sub>2</sub> is the most thermodynamically stable Se-oxide, but it sublimes above 315°C (Dean 1979). Therefore, even if SeO<sub>2</sub> forms, it may partially evaporate from the surface if the oxidation temperature approaches 315°C.

### CdS/CuInSe<sub>2</sub> Interface Formation

#### A. CdS Deposited upon CuInSe<sub>2</sub>

When depositing CdS upon CuInSe<sub>2</sub> various solid-state reactions are conceivable. However, only two reactions were found to be thermodynamically feasible (*i.e.*, having a negative  $\Delta H_R$ ). These reactions are:

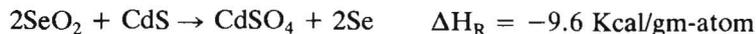


Since these values of  $\Delta H_R$  are very close to zero, there is very little thermodynamic driving force pushing the reaction towards completion. Even the thermodynamic feasibility of these reactions is questionable since the  $\Delta H_R$ 's are within the range of uncertainty inherent in the assumptions of the thermodynamic analysis. The accuracy of the estimated value of  $\Delta H_f^\circ$  for CuInSe<sub>2</sub> makes prediction of the stability of these reactions particularly questionable. Therefore, it does not appear likely that chemical reactions will occur when CdS is deposited upon CuInSe<sub>2</sub> and, if reactions do occur, they will be very weak.

#### B. CdS Deposited upon CuInSe<sub>2</sub> Native Oxides

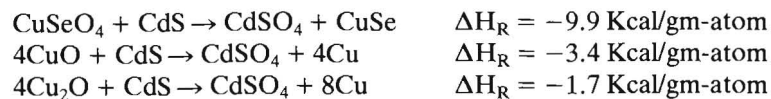
Although CdS/CuInSe<sub>2</sub> heterojunction solar cells are typically fabricated in a vacuum environment, it is conceivable that a thin native oxide could grow upon the CuInSe<sub>2</sub> substrate and CdS would then be deposited upon this native oxide. In this section, we explore the possibility of solid-state reactions occurring between CdS and the native oxide of CuInSe<sub>2</sub>.

Tables 2 and 4 show that the native oxide of CuInSe<sub>2</sub> is usually expected to be composed of In<sub>2</sub>O<sub>3</sub> and SeO<sub>2</sub> (or possibly Se<sub>2</sub>O<sub>5</sub>). A thermodynamic analysis of reactions between CdS and In<sub>2</sub>O<sub>3</sub> indicates that there are no reactions expected between the two. However, if CdS and SeO<sub>2</sub> come into close physical proximity, several reactions are thermodynamically feasible. The most probable reaction was found to be



The general conclusion is that CdS will tend to reduce SeO<sub>2</sub> while CdS and In<sub>2</sub>O<sub>3</sub> will not react.

Native oxides of CuInSe<sub>2</sub> which are thin enough not to be kinetically limited by Cu-diffusion may have CuSeO<sub>2</sub>, CuO, or Cu<sub>2</sub>O also present in the native oxide. When CdS is deposited upon these native oxides, thermodynamic analysis indicates that the following reactions are most probable:



These equations indicate that CdS will tend to oxidize and form CdSO<sub>4</sub> at the expense of reducing the Cu-oxide.

### C. Annealing of CdS/CuInSe<sub>2</sub> Solar Cells in Oxygen

It has been reported that annealing of CdS/CuInSe<sub>2</sub> heterojunction solar cells in oxygen can improve the cell response by increasing the open-circuit voltage and fillfactor (Chen *et al.* 1981). It is possible that this improvement could be associated with oxidation of the CuInSe<sub>2</sub> substrate. However, this appears to be extremely unlikely since oxygen would have to diffuse through several microns of CdS at a relatively low temperature in order to reach the substrate.

It is possible that the oxygen is reacting with the CdS, and this oxidation is partially responsible for the observed improvement in the solar cell response. Thermodynamic analysis indicates that the most probable oxidation reaction would be:



It is possible that the formation of a thin, surface oxide of CdS could reduce the recombination at the solar cell surface, thereby increasing the fill-factor and open-circuit voltage.

Photoconductivity, field effect, and surface photovoltage measurements provide support for this conclusion. Clean CdS surfaces appear to have no intrinsic surface states (Fromhold 1976, Kazmerski *et al.* 1982b) and hence the energy bands are nearly flat. When oxygen is chemisorbed to the surface, extrinsic interface states appear which bend the bands upwards. This band-bending aids minority carrier transport to the CdS surface are nearly flat. When oxygen is chemisorbed to the surface, extrinsic interface states appear which bend the bands upward. Photoconductivity measurements (Kubaschewski *et al.* 1967) using sintered CdS layers indicate that the dark current may be reduced by orders of magnitude by chemisorption of oxygen onto clean CdS surfaces.

### Conclusion

Thermodynamic arguments have been presented which predict the solid-state reaction products for the oxidation of CuInSe<sub>2</sub>, the oxidation of CdS, and for possible reactions at the CdS/CuInSe<sub>2</sub> interface. The approach taken assumes that interfacial reactions can be modelled according to the postulate of local equilibrium and the temperature dependence and entropy component of the Gibbs free energy

may be neglected. With these assumptions in mind, the conclusions are as follows:

1. The reaction products for the situation of fully-oxidized CuInSe<sub>2</sub> with no kinetic limitations are In<sub>2</sub>O<sub>3</sub>, SeO<sub>2</sub> (or possibly Se<sub>2</sub>O<sub>5</sub>) and CuSeO<sub>4</sub>, CuO or Cu<sub>2</sub>O.

2. The reaction products for CuInSe<sub>2</sub> with Cu-diffusion limited are In<sub>2</sub>O<sub>3</sub> and SeO<sub>2</sub> with Cu, Cu<sub>2</sub>Se or CuSe at the interface.

3. For CdS and CuInSe<sub>2</sub>, no reaction occurs or possibly a weak reaction occurs yielding In<sub>2</sub>Se<sub>3</sub>, and CdSe, and Cu<sub>2</sub>S or CuS and Cu.

4. For CdS and the native oxide of CuInSe<sub>2</sub>, no reaction will occur between CdS and In<sub>2</sub>O<sub>3</sub> while any Cu- or Se- oxide within close physical proximity of CdS will be reduced and CdSO<sub>4</sub> will form.

5. CdS is predicted to form CdSO<sub>4</sub> when oxygen is present. It is suggested that the native oxide of CdS may be associated with the improvement of the open-circuit voltage and fill-factor of CdS/CuInSe<sub>2</sub> solar cells upon annealing treatments in oxygen.

It is believed that the thermodynamic approach is a useful conceptual framework for modelling this interface. This analysis may also be useful in conjunction with X-ray photoelectron spectroscopy and Auger electron spectroscopy studies of the chemistry of this system since it eliminates the likelihood of certain reaction products forming and predicts which compounds would be most probable to form.

### References

- Chen, W.S. and Mickelson, R.A.** (1981) *Proc. Soc. Photo Opt. Instrum. Eng.* **248** : 62; Also, **Mickelson, R.A. and Chen, W.S.** (1981) Development of a 9.4% efficient thin-film CuInSe<sub>2</sub>/CdS solar cell, *Proc. 15th IEEE Photovoltaic Spec. Conf., Orlando, FL (IEEE, New York)*, pp. 800-804.
- Dean, J.R., ed.** (1979) *Lange's Handbook of Chemistry*, 12th Ed., McGraw-Hill, New York, pp. 191-200.
- Fromhold, A.T.** (1976) *Theory of Metal Oxidation*, Vol. I, North-Holland, Amsterdam, 65 p.
- Kazmerski, L.L., Ireland, P.J., Jamjoum, O. and Clark, A.H.** (1982a) *Scanning Electron Microscopy/1981/I*, SEM, O'Hare, Illinois, pp. 285-290.
- Kazmerski, L.L., Jamjoum, O., Ireland, P.J., Deb, S.K., Mickelson, R.A. and Chen, W.S.** (1981) Initial oxidation of CuInSe<sub>2</sub>, *J. Vac. Sci. Technol.* **19** : 467-471.
- Kazmerski, L.L., Jamjoum, O., Ireland, P.J., Mickelson, R.A. and Chen, W.S.** (1982b) Formation, growth and stability of the CdS/CuInSe<sub>2</sub> solar cell interfaces, *J. Vac. Sci. Technol.* **21** : 486-490; *idem* (1982b) Annealing and interface effects in CdS/CuInSe<sub>2</sub> solar cells, *J. Vac. Sci. Technol.* **20** : 308-309.
- Kubaschewski, O., Evans, E. and Alcock, C.** (1967) *Metallurgical Thermochemistry*, 4th Ed., Pergamon, Oxford, 123 p.

- Russell, P.E., Jamjoum, O., Ahrenkiel, R.K., Kazmerski, L.L., Mickelson, R.A. and Chen, W.S.** (1982) Properties of the Mo-CuInSe<sub>2</sub> interface, *Appl. Phys. Lett.* **40** : 995-997.
- Welch, A.F.E.** (1955) in: **Garner, W.E. (ed.)** *Chemistry of the Solid State*, Butterworths Sci. Publ., London, p. 76.

*Received 09/03/1983;  
in revised form 14/05/1983)*

## اعتبارات ديناميكية حرارية للحد الفاصل بين كبريتيد الكادميوم (CdS) وثاني سليينات النحاس والإنديوم Cu In Se<sub>2</sub>

ج . ف واجر\* ، أسامة محمد مجموعم\*\* ول . ل . كازمرسكي\*\*\*

\* معامل أبحاث هيوز- مالبو- كاليفورنيا - الولايات المتحدة ؛

\*\* قسم الفيزياء - جامعة الملك عبد العزيز - جدة - المملكة العربية  
السعودية ؛

\*\*\* معهد أبحاث الطاقة الشمسية - جولدن - كلورادو - الولايات  
المتحدة .

يعبر هذا البحث عن مناقشة ديناميكية حرارية لتأكسد ثاني  
سليينات النحاس والإنديوم Cu In Se<sub>2</sub> والتفاعلات الكيميائية  
المتوقعة على الحد الفاصل بين كبريتيد الكادميوم (CdS) وثاني  
سليينات النحاس والإنديوم .

اقترح من خلال هذا العمل عدة تفاعلات كيميائية  
نتيجة لتأكسد ثاني سليينات النحاس والإنديوم وكبريتيد  
الكادميوم . وقد تبين من هذا العمل بعض من التفاعلات  
الكيميائية المتوقع أن تحدث بين كبريتيد الكادميوم وثاني  
سليينات النحاس والإنديوم . ولوحظ من خلال هذا البحث  
أن هناك علاقة بين تأكسد كبريتيد الكادميوم وبين التحسن  
الجزئي في قدرة الخلايا الشمسية المكونة من كبريتيد الكادميوم  
على ثاني سليينات النحاس والإنديوم حين تسخينها في جو من  
الأكسجين .